JOURNAL OF AGRICULTURAL AND FOOD CHEMISTRY

Article

pubs.acs.org/JAFC

Anti-inflammatory and PPAR Transactivational Effects of Components from the Stem Bark of *Ginkgo biloba*

Nguyen Thi Thanh Ngan,[†] Tran Hong Quang,[†,‡] Bui Huu Tai,[†] Seok Bean Song,[†] Dongho Lee,[§] and Young Ho Kim*[,†]

[†]College of Pharmacy, Chungnam National University, Daejeon 305-764, Korea

[‡]Institute of Marine Biochemistry, Vietnam Academy of Science and Technology (VAST), 18 Hoang Quoc Viet, Caugiay, Hanoi, Viet Nam

[§]School of Life Sciences and Biotechnology, Korea University, Seoul 136-713, Korea

Supporting Information

ABSTRACT: *Ginkgo biloba*, which is considered a "living fossil", has been used for medicinal purposes for thousands of years. Currently, extracts of *G. biloba* are some of the most widely used herbal products and/or dietary supplements in the world. In this study, three new compounds, (2*E*,4*E*,1′*R*,3′*S*,5′*R*,8′*S*)-dihydrophaseic acid 3′-*O*-*β*-D-glucopyranoside (**1**), 7,8-dihydro-(*R*)-7-methoxyconiferyl alcohol (**2**), and (8*S*)-3-methoxy-8,4′-oxyneolignan-4,9,9′-triol 3′-*O*-*β*-D-glucopyranoside (**3**), and 13 known compounds (**4**−**16**) were isolated from the stem bark of *G. biloba*. Their structures were determined by extensive spectroscopic methods, including 1D and 2D NMR, MS, and circular dichroism spectra. Four of the compounds (**1**, **2**, **7**, and **10**) inhibited TNF*α*-induced NF-*κ*B transcriptional activity significantly in HepG2 cells in a dose-dependent manner, with IC_{50} values ranging from 6.9 to 9.1 *μ*M. Furthermore, the transcriptional inhibitory function of these compounds was confirmed based on decreases in COX-2 and iNOS gene expression in HepG2 cells. Compounds **1**−**5**, **7**, **9**, **10**, and **12**−**14** significantly activated the transcriptional activity of PPARs in a dose-dependent manner, with EC_{50} values ranging from 0.7 to 12.8 *μ*M. Compounds **2**, **3**, and **12** exhibited dose-dependent PPAR*α* transactivational activity, with EC_{50} values of 7.0, 3.3, and 10.1 *μ*M, respectively. Compounds **1**−**3** activated PPAR*γ* transcriptional activity, with EC_{50} values of 11.9, 11.0, and 15.3 *μ*M, whereas compounds **1** and **3** promoted the transactivational activity of PPAR*β*(*δ*) with EC_{50} values of 10.7 and 11.2 *μ*M, respectively. These results provide a scientific support for the use of *G. biloba* stem bark for the prevention and treatment of inflammatory and metabolic diseases. Moreover, these data provide the rationale for further studies of the potential of *G. biloba* stem bark in functional foods.

KEYWORDS: *Ginkgo biloba, NF-κB-luciferase assay, RT-PCR, PPRE-luciferase assay, GAL-4-PPAR chimera assay*

INTRODUCTION

Ginkgo biloba, the only surviving member of the Ginkgoaceae family, exhibits many remarkable pharmacological and clinical effects, and it is the most frequently used product as a phytomedicine in many countries. Numerous studies have shown that Ginkgo extracts possess many pharmacological properties, including radical scavenging, improvement of blood flow, vasoprotection, cognitive enhancement, and antiplatelet-activating factor activities.[1,2] The Ginkgo tree has been widely cultivated since an early period in human history and has been used in various foods and traditional medicines. As reported by Singh et al., over seven billion dollars are spent annually on botanical medicines, and *G. biloba* ranks first among herbal medications.[3] The use of *G. biloba* has been growing at a rapid rate of 25% per year in the open world commercial market. In 2008, there were around 142 *G. biloba* products on the global market, and the utilization of *G. biloba* is still increasing.[3] Currently, *G. biloba* is one of the most widely used herbal products and/or dietary supplements in the world.[4] Extracts of *G. biloba* leaves have been reported to possess a number of secondary metabolites, including terpenoids (notably ginkgolides and bilobalide), polyphenols, allyl phenols, organic acids, carbohydrates, fatty acids, and lipids.[3] However, few chemical investigations of *G. biloba* stem bark have been reported. This report describes the isolation and structural elucidation of three new (**1**−**3**) and 13 known compounds (**4**−**16**) from the methanol extract of the stem bark of *G. biloba*.

Nuclear factor-*κ*B (NF-*κ*B) is an inducible transcription factor of the Rel family. The activation of NF-*κ*B by stimuli, including inflammatory cytokines such as tumor necrosis factor *α* (TNF-*α*) and IL-1, T-cell activation signals, growth factors, and stress inducers causes transcription at *κ*B sites. This transcription is involved in a number of diseases, including cancer, AIDS, and inflammatory disorders.[5,6] Hence, the inhibition of NF-*κ*B signaling has become a therapeutic target for treating inflammatory diseases and cancer. The effects of compounds **1**−**17** on TNF*α*-induced NF-*κ*B transcriptional activity in human hepatocarcinoma (HepG2) cells were evaluated using an NF-*κ*B-luciferase assay. To confirm the inhibitory effects of the compounds on NF-*κ*B transcriptional activity, the effects of the isolated compounds on the upregulation of the pro-inflammatory proteins inducible nitric oxide synthase (iNOS) and cyclooxygenase-2 (COX-2) were

Received: November 21, 2011
Revised: February 13, 2012
Accepted: February 21, 2012
Published: February 21, 2012

Table 1. ^{1}H and ^{13}C NMR Data for Compounds 1−3[a]

	1		2		3	
position	δ_H[b]	δ_C[c]	δ_H[d]	δ_C[e]	δ_H[d]	δ_C[e]
1		175.0		133.6		130.8
2	5.81 s	127.9	6.83 d (1.8)	110.0	6.79 d (1.2)	114.2
3		139.2		148.3		148.8
4	7.69 d (16.0)	132.3		146.3		146.0
5	6.21 d (16.0)	129.0	6.74 d (7.8)	115.1	6.68 d (7.8)	116.1
6	1.91 s	19.5	6.71 dd (7.8, 1.8)	119.8	6.69 d (7.8)	123.0
7			4.20 dd (8.4, 6.0)	81.2	2.92 d (14.4, 7.2)	37.5
					2.86 d (13.8, 7.2)	
8			1.96 m	41.1	4.36 m	84.2
			1.74 m			
9			3.58 m	58.9	3.68 m	63.7
			3.49 m		3.58 dd (12.0, 4.8)	
3-OCH_3			3.81 s	55.4	3.91 s	56.4
7-OCH_3			3.14 s	55.6		
1′		48.3				137.9
2′	2.13 m	41.9			7.04 br s	120.6
	1.80 m					
3′	4.20 m	73.2				149.4
4′	1.93 m	41.9				147.8
	1.75 m					
5′		86.7			6.76 d (7.8)	119.7
6′					6.76 d (7.8)	124.5
7′	3.77 m	76.3			2.57 m	32.3
	3.70 m					
8′		82.2			1.76 m	35.2
9′	1.13 s	18.8			3.67 m	62.1
					3.51 m	
10′	0.90 s	15.4				
1″	4.33 d (8.0)	102.3			4.81 d (7.8)	103.5
2″	3.11 dd (9.6, 8.0)	74.2			3.46 dd (8.4, 7.8)	75.0
3″	3.24 dd (9.6, 8.4)	77.2			3.43 dd (9.0, 8.4)	77.8
4″	3.25 dd (8.4, 8.0)	70.8			3.37 dd (8.4, 7.8)	71.3
5″	3.32 m	77.0			3.33 m	78.1
6″	3.83 dd (11.6, 2.0)	61.9			3.84 m	62.4
	3.64 dd (11.6, 1.6)				3.67 m	

[a]Coupling constants (J) are in Hz. Assignments were confirmed by HMQC, HMBC, and NOESY spectra. [b]Spectra were recorded in methanol-d_4 at 400 MHz. [c]Spectra were recorded in methanol-d_4 at 100 MHz. [d]Spectra were recorded in methanol-d_4 at 600 MHz. [e]Spectra were recorded in methanol-d_4 at 150 MHz.

evaluated in TNFα-stimulated HepG2 cells by reverse transcriptase polymerase chain reaction (RT-PCR).

Peroxisome proliferator-activated receptors (PPARs) comprise a subfamily of the nuclear receptor superfamily, of which three isoforms, PPARα, PPARγ, and PPAR$\beta(\delta)$, have been identified. PPARs regulate the expression of genes involved in the regulation of glucose, lipid, and cholesterol metabolism by binding to specific peroxisome proliferator response elements (PPREs) in the enhancer sites of regulated genes.[7−10] Accordingly, compounds that modulate the functions of PPARs are attractive for the treatment of type 2 diabetes, obesity, metabolic syndromes, inflammation, and cardiovascular disease.[11] Thus, we initially investigated the effects of compounds **1**−**17** on the transcriptional activity of PPARs in HepG2 cells using a PPRE-luciferase assay. Although the PPAR subtypes share a high level of sequence and structural homology, each has distinct physiological functions and exhibits a unique tissue expression pattern.[12] Thus, with the aim of understanding exactly how these compounds modulate PPAR transcriptional activity, we further examined the transactivational effects of the compounds on the individual PPAR subtypes, PPARα, -γ, and -$\beta(\delta)$, using GAL-4-PPAR chimera assays.

MATERIALS AND METHODS

General Procedures. Optical rotations were determined using a Jasco P-2000 digital polarimeter. The Fourier transform infrared (FT-IR) spectra were measured using a Nicolet 380 FTIR spectrometer. Electrospray ionization (ESI) mass spectra were obtained using an Agilent 1200 LC-MSD Trap spectrometer. GC was carried out on a Shidmazu-2010 spectrometer. High-resolution ESI time-of-flight mass spectra (HRESITOFMS) were obtained using an Acquity UPLC system (Waters, Milford, MA) with a Micromass Q-Tof Micro mass spectrometer (Waters, Manchester, United Kingdom). The NMR spectra were recorded on JEOL ECA 400 and 600 spectrometers using TMS as an internal standard. Circular dichroism (CD) spectra were recorded with a Jasco J-720 spectropolarimeter. Thin-layer chromatography (TLC) was performed on Kieselgel 60 F_{254} (1.05715; Merck, Darmstadt, Germany) or RP-18 F_{254s} (Merck) plates. Spots were visualized by spraying with 10% aqueous H_2SO_4 solution, followed by heating. Column chromatography was performed on silica gel

(Kieselgel 60, 70−230 mesh and 230−400 mesh, Merck) and YMC RP-18 resins.

Plant Material. The stem bark of of *G. biloba* was collected at Muju, Chungnam, Korea, in August, 2010. The plant material was identified by Y. H. Kim. A voucher specimen (CNU10104) was deposited at herbarium, College of Pharmacy, Chungnam National University.

Extraction and Isolation. The dried stem bark of *G. biloba* (5 kg) was extracted with hot MeOH. After concentration, the MeOH extract (250 g) was suspended in H_2O and then partitioned successively with *n*-hexane, CH_2Cl_2, and EtOAc to give *n*-hexane (A, 35 g), CH_2Cl_2 (B, 60 g), EtOAc (C, 20 g), and aqueous (D, 135 g) fractions, respectively. Fraction B was chromatographed over silica gel, eluting with acetone in *n*-hexane (0−100%, stepwise), to give five fractions (B1−B5). Fraction B3 (6 g) was subjected to an YMC RP column chromatography (CC) using MeOH−H_2O (3:1) as eluents and further purified over silica gel column eluting with CH_2Cl_2−EtOAc (7:1), to afford **2** (5 mg) and **4** (20 mg). Fraction B4 (18 g) was chromatographed over a silica gel column eluting with *n*-hexane−acetone (1:1) to obtain three subfractions B4.1−B4.3. Subfraction B4.1 (5 g) was then chromatographed over a silica gel column, using CH_2Cl_2−acetone (7:1) as eluents to give **14** (8 mg). Compounds **9** (7 mg) and **15** (12 mg) were isolated from subfraction B4.2 (8 g) by CC over silica gel, eluted with CH_2Cl_2−EtOAc (5:1). Subfraction B4.3 (3.7 g) was chromatographed over YMC RP, using acetone−H_2O (1:1) to afford **11** (9 mg). B5 (3 g) was separated by an YMC RP CC, eluting with acetone−H_2O (1:1) to yield **7** (30 mg) and **10** (10 mg). Fraction C was subjected to a silica gel column, eluting with MeOH in CH_2Cl_2 (0−100%, stepwise) to provide three subfractions (C1−C3). Subfraction C2 (7 g) was separated by an YMC RP CC, using MeOH−H_2O (1:1) as eluents and further purified by CC over silica gel, eluting with CH_2Cl_2−acetone (2:1) to obtain **13** (32 mg). The aqueous fraction D was chromatographed on a column of highly porous polymer (Diaion HP-20) and eluted with H_2O and MeOH, successively to give three fractions (D1−D3). Fraction D2 (27 g) was chromatographed over silica gel, eluting with MeOH in CH_2Cl_2 (0−100%, stepwise) to provide five subfractions (D2.1−D2.5). Subfraction D2.2 (2.3 g) was separated by an YMC RP CC, using MeOH−H_2O (1:1) as eluents, and further purified by CC over silica gel, eluting with CH_2Cl_2−MeOH (10:1) to obtain **16** (15 mg). Subfraction D2.3 (3.8 g) was separated by CC over silica gel, using CH_2Cl_2−MeOH−H_2O (5:1:0.1) as eluents, and further purified by YMC RP chromatography, eluting with MeOH−H_2O (1:1) to give **1** (5 mg) and **5** (20 mg). From subfraction D2.4 (2.2 g), **6** (5 mg) was isolated by silica gel CC, eluting with CH_2Cl_2−MeOH−H_2O (6:1:0.1). Fraction D2.5 (4.3 g) was chromatographed over silica gel, eluting with CH_2Cl_2−MeOH−H_2O (5:1:0.1) to provide **3** (15 mg) and **12** (11 mg). Subfraction D3 (6 g) was separated by CC over silica gel, eluting with CH_2Cl_2−MeOH−H_2O (3:1:0.1), and further purified by an YMC RP CC, using MeOH−H_2O (1:2) as eluents, to obtain **8** (55 mg).

*(2E,4E,1′R,3′S,5′R,8′S)-Dihydrophaseic Acid 3′-O-β-D-Glucopyranoside (**1**).* Colorless gum; $[\alpha]_D^{25}$ − 17.6 (*c* 0.3, MeOH). FT-IR (CH_3CN) ν_{max} 3369, 2930, 2876, 1602, 1560, 1400, 1336, 1074, 1021, and 884 cm^{-1}. HRESITOFMS *m*/*z* 443.1896 $[M - H]^-$ (calcd for $C_{21}H_{31}O_{10}$, 443.1917). CD (MeOH) nm ($\Delta\varepsilon$): 237.4 (− 9.39). ^1H (methanol-d_4, 400 MHz) and ^{13}C NMR data (methanol-d_4, 150 MHz), see Table 1.

*7,8-Dihydro-(R)-7-methoxyconiferyl Alcohol (**2**).* White, amorphous powder; $[\alpha]_D^{25}$ + 9.0 (*c* 0.12, MeOH). FT-IR (CH_3CN) ν_{max} 3287, 2936, 1602, 1516, 1272, 1033, 821 cm^{-1}. HRESITOFMS *m*/*z* 211.0985 $[M - H]^-$ (calcd for $C_{11}H_{15}O_4$, 211.0970). ^1H NMR data (methanol-d_4, 600 MHz) and ^{13}C NMR data (methanol-d_4, 150 MHz), see Table 1.

*(8S)-3-Methoxy-8,4′-oxyneolignan-4,9,9′-triol 3′-O-β-D-Glucopyranoside (**3**).* White, amorphous powder; $[\alpha]_D^{25}$ − 17.6 (*c* 0.3, MeOH). FT-IR (CH_3CN) ν_{max} 3361, 2937, 1602, 1513, 1267, 1070, 1033 cm^{-1}. HRESITOFMS *m*/*z* 509.2038 $[M - H]^-$ (calcd for $C_{25}H_{33}O_{11}$, 509.2023). CD (MeOH) nm ($\Delta\varepsilon$): 238.6 (+10.34). ^1H NMR data (methanol-d_4, 600 MHz) and ^{13}C NMR data (methanol-d_4, 150 MHz), see Table 1.

Acid Hydrolysis and Sugar Identification. Each compound (2 mg) was heated in 3 mL of 10% HCl−dioxane (1:1) at 80 °C for 3 h. After the solvent was removed in vacuo, the residue was partitioned between EtOAc and H_2O to give the aglycone and sugar, respectively. The sugar in the aqueous layer was analyzed by silica gel TLC by comparison with standard sugars. The solvent system was CH_2Cl_2−MeOH−H_2O (2:1:0.2), and spots were visualized by spraying with 95% EtOH−H_2SO_4−anisaldehyde (9:0.5:0.5, v/v) and then heated at 150 °C for 5 min. The R_f value of glucose by TLC was 0.30. The result was confirmed by GC analysis. The aqueous layer was evaporated to dryness to give a residue and was dissolved in anhydrous pyridine (100 μL) and then mixed with a pyridine solution of 0.1 M L-cysteine methyl ester hydrochloride (100 μL). After the mixture was warmed at 60 °C for 2 h, trimethylsilylimidazole solution was added and warmed at 60 °C for 2 h. The mixture was evaporated in vacuo to give a dried product, which was partitioned between *n*-hexane and H_2O. The *n*-hexane layer was filtered and analyzed by GC under following conditions: detector, FID; detection temperature, 300 °C; column, SPB-1 (0.25 mm i.d. × 30 m); column temperature, 230 °C; He carrier gas (2 mL/min); injection temperature, 250 °C; and injection volume, 0.5 μL. The retention time of the persilylated sugar was detected at t_R = 14.12 min for D-glucose, as compared with those of authentic standards (Sigma) [D-glucose (t_R, 14.12 min) and L-glucose (t_R, 14.25 min)].

Cell Culture and Reagents. Human hepatocarcinoma HepG2 cells were maintained in Dulbecco's modified Eagles' medium (DMEM) (Invitrogen, Carlsbad, CA) containing 10% heat-inactivated fetal bovine serum (FBS), 100 units/mL penicillin, and 10 μg/mL streptomycin at 37 °C and 5% CO_2.

NF-κB-Luciferase Assay. The luciferase vector was first transfected into HepG2 cells. After a limited amount of time, the cells were lysed, and luciferin, the substrate of luciferase, was introduced into the cellular extract along with Mg^{2+} and an excess of ATP. Under these conditions, luciferase enzymes expressed by the reporter vector could catalyze the oxidative carboxylation of luciferin. Cells were seeded at 1.5×10^5 cells per well in 12-well plates and grown for 24 h. All cells were transfected using WelFect M Gold (WelGENE Inc.), as guided by the manufacturer. The luciferase activity was assayed using an LB 953 Autolumat (EG&G Berthold, Nashua, NH).[13] The transfected HepG2 cells were pretreated for 1 h with either vehicle (DMSO) and compounds, followed by 1 h of treatment with 10 ng/mL TNFα. Unstimulated HepG2 cells were used as a negative control (−). Cells were then harvested, and the luciferase activity was assayed.

RNA Preparation and RT-PCR. Total RNA was extracted using Easy-blue reagent (Intron Biotechnology, Seoul, Korea). Approximately 2 μg of total RNA was subjected to reverse transcription using Moloney murine leukemia virus (MMLV) reverse transcriptase and oligo-dT primers (Promega, Madison, WI) for 1 h at 42 °C. PCR for synthetic cDNA was performed using a Taq polymerase premixture (TaKaRa, Japan). The PCR products were separated by electrophoresis on 1% agarose gels and stained with EtBr. PCR was conducted with the following primer pairs: iNOS sense, 5′-TCATCCGCTATGCTGGCTAC-3′; iNOS antisense, 5′-CTCAGGGTCACGGCCATTG-3′; COX-2 sense, 5′-GCCCAG-CACTTCACGCATCAG-3′; COX-2 antisense, 5′-GACCAGGCAC-CAGACCAAAGACC-3′; β-actin sense, 5′-TCACCCA-CACTGTGCCCATCTACG-3′; and β-actin antisense, 5′-CAGCG-GAACCGCTCATTGCCAATG-3′. The specificity of products generated by each set of primers was examined using gel electrophoresis and further confirmed by a melting curve analysis.

HepG2 cells were pretreated in the absence and presence of compounds for 1 h and then exposed to 10 ng/mL TNFα for 6 h. The total mRNA was prepared from the cell pellets using Easy-blue. The levels of mRNA were assessed by RT-PCR.

PPRE-Luciferase Assay. Human hepatoma cells (HepG2) were seeded at 1.5×10^5 cells per well in 12-well plates and grown for 24 h before transfection. An optimized amount of DNA plasmid (0.5 μg of PPRE-Luc and 0.2 μg of PPAR-inpCMV) was diluted in 100 μL of DMEM. All cells were transfected with the plasmid mixture using WelFect M Gold (WelGENE Inc.) as described by the manufacturer.

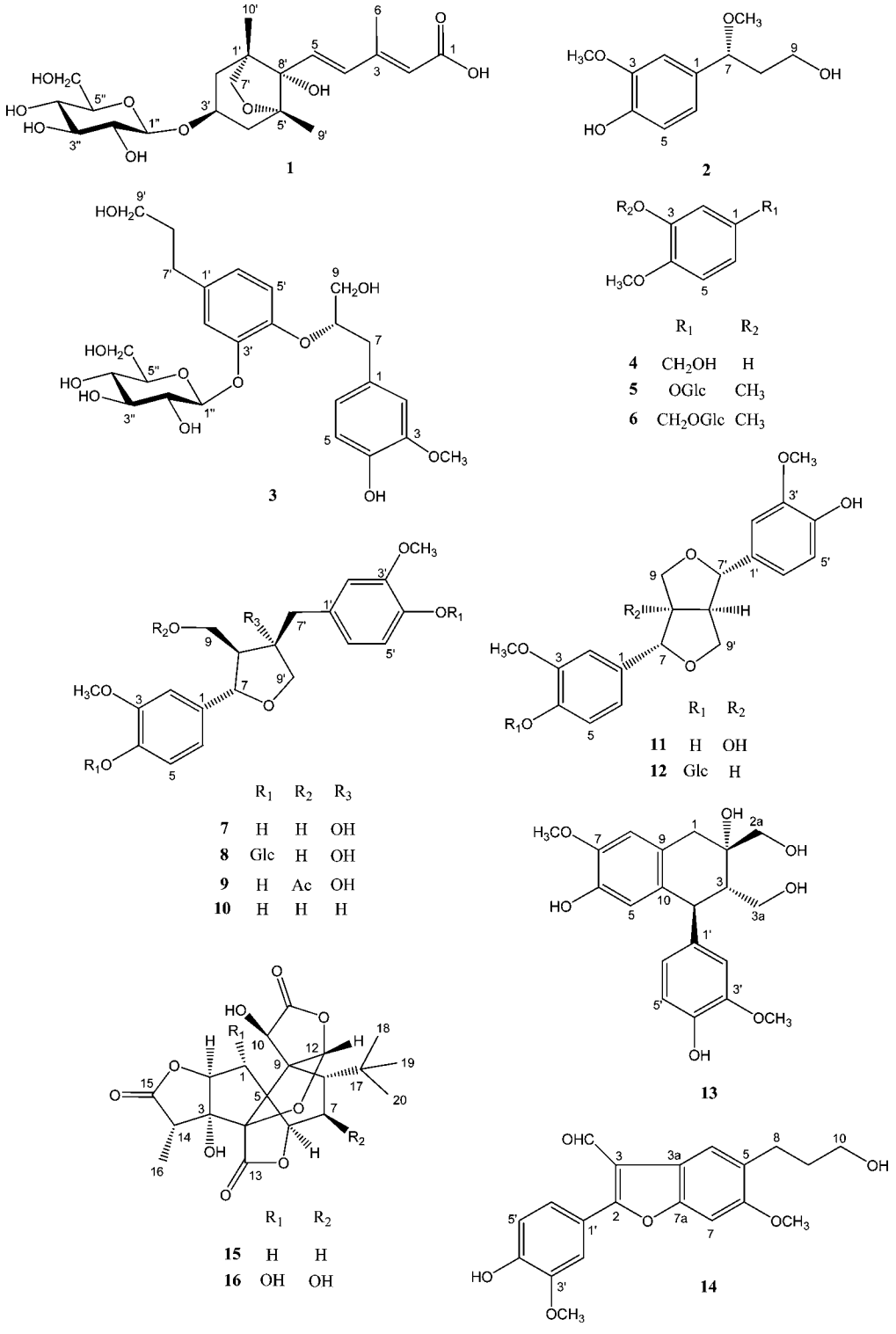

Figure 1. Structure of compounds **1**−**16**.

After 30 min of incubation at room temperature, the DNA plasmid solution (100 μL) was introduced and mixed gently with cells. After 24 h of transfection, the medium was changed to TOM (Transfection Optimized Medium, Invitrogen) containing 0.1 mM NEAA, 0.5% charcoal- stripped FBS, and the individual compounds (test group), dimethyl sulfoxide (vehicle group), or benzafibrate (positive control group). The cells were then cultured for 20 h. Next, the cells were washed with PBS and harvested with 1× passive lysis buffer (200 μL). The intensity of emitted luminescence was determined using an LB 953 Autolumat (EG&G Berthold, Bad Wildbad, Germany).

PPAR Subtype Specific Transactivational Assay. Human hepatoma cells (HepG2) were seeded at 1.5×10^5 cells per well in 12-well plates and grown for 24 h before transfection. Cells were transfected separately with one pGal4-PPAR subfamily vector [pFA-Gal4-PPARα-LBD, pFA-Gal4-PPARγ-LBD, or pFA-Gal4-PPAR$\beta(\delta)$-LBD expression plasmids], together with pFR-Luc using the WelFect M Gold transfection reagent (WelGENE Inc.), as described by the manufacturer. After 24 h of transfection, the medium was changed to TOM (Invitrogen) containing 0.1 mM NEAA, 0.5% charcoal-stripped FBS, and each compound (test group), dimethyl sulfoxide (vehicle

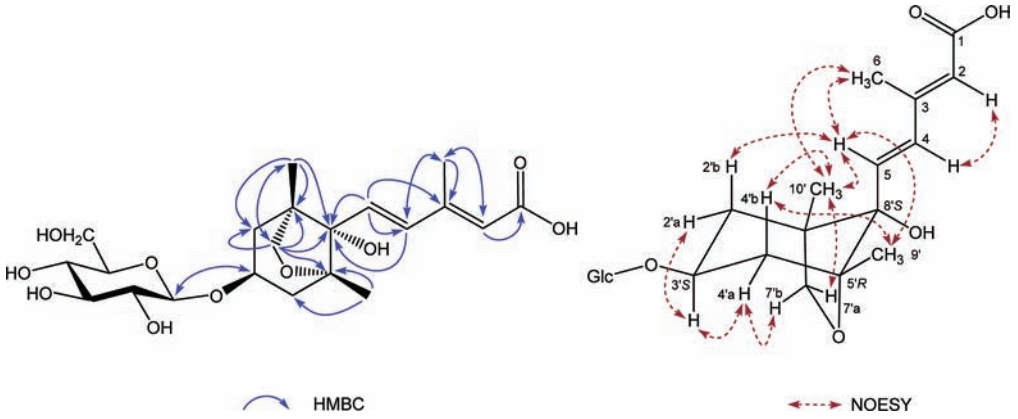

Figure 2. Selected HMBC and NOESY correlations of compound **1**.

group), ciprofibrate (positive control group for PPARα), troglitazone (positive control group for PPARγ), or L-165041 [positive control group for PPAR$\beta(\delta)$]. The cells were then cultured for 20 h, after which the cells were washed with PBS and harvested with 1× passive lysis buffer (200 μL). The intensity of emitted luminescence was determined using a Centro LB 960 microplate luminometer (EG&G Berthold) by measuring light emission for 5 s.

Statistical Analysis. All data represent the mean ± standard deviation (SD) of at least three independent experiments performed in triplicate. Statistical significance is indicated as * ($p < 0.05$) as determined by one-way analysis of variance followed by Dunnett's multiple comparison test.

RESULTS AND DISCUSSION

Isolation and Structure Elucidation of Compounds. A MeOH extract of the dried stem bark of *G. biloba* (250 g) was suspended in H_2O and successively extracted with *n*-hexane, CH_2Cl_2, and EtOAc. The CH_2Cl_2-, EtOAc-, and H_2O-soluble fractions were subjected to multiple chromatographic steps over Diaion HP-20, silica gel, and reversed-phase C_{18}, yielding compounds **1**−**16**. Comparison of the NMR and MS data with reported values in the literature led to identification of the structures of the known compounds to be vanillyl alcohol (**4**),[14] 3,4-dimethoxyphenyl β-D-glucopyranoside (**5**),[15] 3,4-dimethoxyphenyl alcohol-7-*O*-β-D-glucopyranoside (**6**),[16] olivil (**7**),[17] (−)-olivil 4,4′-di-*O*-β-D-glucopyranoside (**8**),[18] lariresinol (**9**),[19] (+)-lariciresinol (**10**),[20] (+)-8-hydroxypinoresinol (**11**),[17] (+)-pinoresinol *O*-β-D-glucopyranoside (**12**),[21] (+)-cycloolivil (**13**),[22] 5-(3-hydroxypropyl)-6-methoxy-2-(3′-methoxy-4′-hydroxyphenyl)-3-benzofurancarboxaldehyde (**14**),[23] ginkgolide A (**15**),[24] and ginkgolide C (**16**)[24] (Figure 1).

Compound **1** was isolated as a colorless gum. The molecular formula of **1** was determined to be $C_{21}H_{32}O_{10}$ from a pseudomolecular ion peak $[M - H]^-$ at *m*/*z* 443.1896 (calcd for $C_{21}H_{31}O_{10}$, 443.1917) in the HRESITOFMS. The ^{1}H NMR spectrum (Table 1) of **1** exhibited three tertiary methyl singlets at δ_H 1.91 (Me-6), 1.13 (Me-9′), and 0.90 (Me-10′) and three signals of olefinic protons at δ_H 5.81 (1H, s, H-2), 7.69 (1H, d, J = 16.0 Hz, H-4), and 6.21 (1H, d, J = 16.0 Hz, H-5). The large coupling constant (J = 16.0 Hz) of the two olefinic protons indicated a *trans*-configured double bond. The ^{1}H NMR spectrum of **1** further showed the signal of an anomeric proton at δ_H 4.33 (1H, d, J = 8.0 Hz, H-1″), indicating the presence of a sugar moiety. Acid hydrolysis of **1** with 10% HCl led to the identification of the sugar as D-glucose. The ^{13}C NMR and DEPT spectra indicated 21 carbons, including three methyl, four methylene, nine methine, and five quaternary carbons. The ^{13}C NMR spectrum (Table 1) of **1** exhibited signals due to a carboxyl carbon (δ_C 175.0, C-1), two double bonds [(δ_C 127.9, C-2), (δ_C 139.2, C-3), (δ_C 132.3, C-4), and (δ_C 129.0, C-5)], two oxygenated quaternary carbons [(δ_C 86.7, C-5′) and (δ_C 82.2, C-8′)], two oxymethylenes [(δ_C 76.3, C-7′) and (δ_C 61.9, C-6″)], and six oxymethines [(δ_C 73.2, C-3′), (δ_C 102.3, C-1″), (δ_C 74.2, C-2″), (δ_C 77.2, C-3″), (δ_C 70.8, C-4″), and (δ_C 77.0, C-5″)]. The position of the oxymethylene group at C-7′ was based on the cross-peaks from H_2-7′ (δ_H 3.77 and 3.70) to C-1′ (δ_C 48.3), C-2′ (δ_C 41.9), C-5′ (δ_C 86.7), C-8′ (δ_C 82.2), and C-10′ (δ_C 15.4) in the HMBC spectrum of **1** (Figure 2). Furthermore, the HMBC correlation of the anomeric proton H-1″ with C-3′ revealed that the glucose moiety was connected to the hydroxyl group at C-3′ of the aglycone. A comparison of the NMR data for **1** (Table 1) with that of *epi*-dihydrophaseic acid-β-D-glucoside[25] revealed that the structures of the two compounds were nearly identical, except for the configurations at C-3′ and a double bond at C-2. The clear differences between the ^{13}C NMR chemical shifts for C-2 (δ_C 127.9) and C-3 (δ_C 139.2) in **1** with respect to those in *epi*-dihydrophaseic acid-β-D-glucoside,[25] together with the good agreement with the reported values for acetylated glucoside of *trans*-abscisic alcohol,[26] indicated a *trans*-configuration at the double bond at C-2 in **1**. This was confirmed by NOE correlations between H-2/H-4 and H-6/H-5 in the NOESY spectrum of **1** (Figure 2). H_3-10′ and H_3-9′ showed NOE correlations with H-5, indicating an α-orientation of the hydroxyl group at C-8′. Furthermore, NOE cross-peaks between H_3-10′/H-4′b, H-5/H-2′b, H-2′a/H-3′, and H-3′/H-4′a suggested an α-orientation of H-3′. On the basis of the above data and a comparison of the CD spectrum of **1** with that of (1′*R*,3′*R*,5′*R*,8′*S*)-*epi*-dihydrophaseic acid β-D-glucoside,[25] the structure of compound **1** was established as (2*E*,4*E*,1′*R*,3′*S*,5′*R*,8′*S*)-dihydrophaseic acid 3′-*O*-β-D-glucopyranoside.

Compound **2** was obtained as an amorphous powder. The HRESITOFMS of **2** exhibited a pseudomolecular ion peak at *m*/*z* 211.0985 $[M - H]^-$ (calcd for $C_{11}H_{15}O_4$, 211.0970), consistent with the molecular formula of $C_{11}H_{16}O_4$. The ^{1}H NMR spectrum of **2** (Table 1) showed signals characteristic of an ABX spin system [δ_H 6.83 (1H, d, J = 1.8 Hz, H-2), 6.74 (1H, d, J = 7.8 Hz, H-5), and 6.71 (1H, dd, J = 7.8, 1.8 Hz, H-6)], revealing the presence of a trisubstituted aromatic ring. The ^{1}H NMR spectrum further exhibited signals corresponding to two methoxyl groups at δ_H 3.81 (3H, s) and 3.14 (3H, s) and one oxymethine group at δ_H 4.20 (1H, dd, J = 8.4, 6.0 Hz, H-

dx.doi.org/10.1021/jf204768d | J. Agric. Food Chem. 2012, 60, 2815−2824

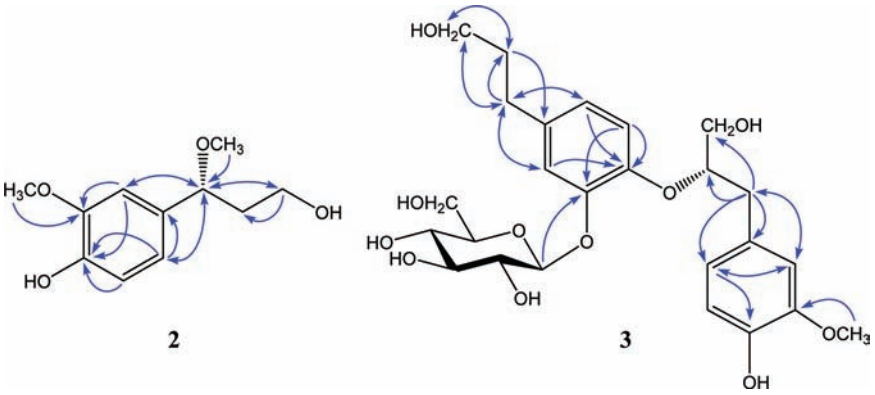

Figure 3. Selected HMBC correlations of compounds **2** and **3**.

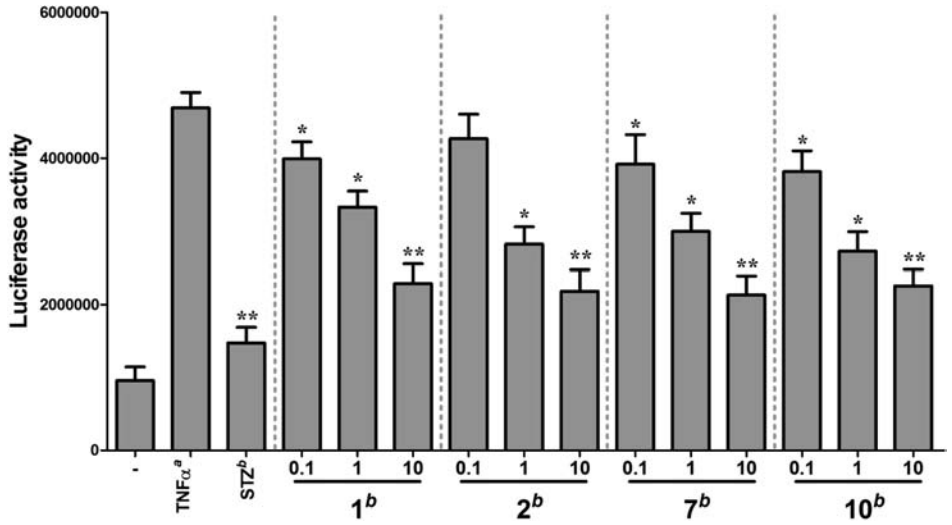

Figure 4. Effects of compounds **1**, **2**, **7**, and **10** on the TNFα-induced NF-κB luciferase reporter activity in HepG2 cells. The values are means ± SDs (n = 3). [a]Stimulated with TNFα. [b]Stimulated with TNFα in the presence of **1**, **2**, **7**, and **10** (0.1, 1, and 10 μM) and sulfasalazine. SFZ: sulfasalazine, positive control (10 μM). Statistical significance is indicated as * (p < 0.05) and ** (p < 0.01) as determined by Dunnett's multiple comparison test.

7). The ^{13}C and DEPT spectra indicated the presence of 11 carbons, including two methyl, two methylene, four methine, and three quaternary carbons. The ^{13}C NMR spectrum (Table 1) exhibited signals due to one oxymethylene group at δ_C 58.9 (C-9), one methylene group at δ_C 41.1 (C-8), one quaternary carbon at δ_C 133.6 (C-1), and two oxygenated quaternary carbons at δ_C 148.3 (C-3) and 146.3 (C-4) of the aromatic ring. In the HMBC spectrum (Figure 3), the signals at δ_H 4.20 (H-7) showed correlations with δ_C 55.6 (a methoxyl carbon), δ_C 133.6 (C-1), 110.0 (C-2), 41.1 (C-8), and 58.9 (C-9), indicating the partial structure of a $-CH(OCH_3)-CH_2-CH_2OH$ moiety connected to the aromatic ring. The position of the methoxyl group at C-3 was confirmed by HMBC correlation between the peaks at δ_H 3.81 and δ_C 148.3 (C-3). The stereochemistry at C-7 was determined as *R* by the positive optical rotation value of **2** ($[\alpha]_D$ + 9.0).[27] Thus, the structure of compound **2** was identified as 7,8-dihydro-(*R*)-7-methoxyconiferyl alcohol.

Compound **3** was obtained as an amorphous powder with a molecular formula of $C_{25}H_{34}O_{11}$, indicated by a pseudomolecular ion peak m/z at 509.2038 $[M - H]^-$ (calcd for $C_{25}H_{33}O_{11}$, 509.2023) in the HRESITOFMS. The ^{1}H NMR spectrum of **3** (Table 1) showed the signals characteristic of two trisubstituted phenyl rings with ABX spin system [δ_H 6.79 (1H, d, J = 1.2 Hz, H-2), 6.68 (1H, d, J = 7.8 Hz, H-5), 6.69 (1H, d, J = 7.8 Hz, H-6), 7.04 (1H, br s, H-2′), and 6.76 (2H, each d, J = 7.8 Hz, H-5′ and H-6′)], one methoxyl group at δ_H 3.91 (3H, s), and one anomeric proton at δ_H 4.81 (1H, d, J = 7.8 Hz, H-1″). These data indicated the presence of a single sugar moiety. The sugar was D-glucose, as determined by acid hydrolysis followed by GC analysis. The ^{13}C NMR and DEPT spectra displayed the presence of 25 carbon signals, including one methyl, six methylene, 12 methine, and six quaternary carbons. The ^{13}C NMR spectrum of **3** (Table 1) showed signals corresponding to three methylene groups at δ_C 37.5 (C-7), 32.3 (C-7′), and 35.2 (C-8′), three oxymethylene groups at δ_C 63.7 (C-9), 62.1 (C-9′), and 62.4 (C-6″), and six oxymethine groups at δ_C 84.2 (C-8), 103.5 (C-1″), 75.0 (C-2″), 77.8 (C-3″), 71.3 (C-4″), and 78.1 (C-5″). These data suggested the presence of two C_6-C_3 units, a neolignan, and a glucopyranose. The glucopyranosyl moiety was linked to the C-3′ hydroxyl group based on an HMBC correlation between the anomeric proton (δ_H 4.81, H-1″) and δ_C 149.4 (C-3′) (Figure 3). On the basis of these analyses and a comparison of the NMR data for **3** with that of related compounds, the planar structure of **3** was established. The absolute configuration of C-8 was determined by CD spectroscopy. The CD spectrum of **3** showed a positive Cotton effect in the region of 238.6 nm ($\Delta\varepsilon$ + 10.34), establishing the (*S*)-configuration at C-8.[28] Finally, the structure of **3** was identified as (8*S*)-3-methoxy-8,4′-oxyneolignan-4,9,9′-triol 3′-*O*-β-D-glucopyranoside.

The anti-inflammatory activity of compounds **1**−**16** was evaluated through inhibition of a TNFα-induced NF-κB luciferase reporter and by the attenuation of TNFα-induced pro-inflammatory gene (iNOS and COX-2) expression in HepG2 cells. The results showed that compounds **1**, **2**, **7**, and **10** significantly inhibited TNFα-induced NF-κB transcriptional activity in HepG2 cells in a dose-dependent manner (Figure 4), with IC_{50} values ranging from 6.9 to 9.1 μM (Table 2). Because

Table 2. Inhibitory Effects of Compounds 1−16 on the TNFα-Induced NF-κB Transcriptional Activity[a]

compd	IC_{50} (μM)
1	9.1 ± 2.4
2	6.9 ± 0.9
7	7.7 ± 1.5
10	7.1 ± 2.0
sufasalazine	0.9 ± 0.1

[a]The values are means ± SDs (n = 3). Compounds **3**−**6**, **8**, **9**, and **11**−**16** were inactive at tested concentrations.

NF-κB is an important transcription factor involved in regulating the expression of inflammatory NF-κB target genes such as iNOS and COX-2,[29,30] we investigated the effects of compounds **1**, **2**, **7**, and **10** on the expression of these genes in TNFα-stimulated HepG2 cells using RT-PCR. Consistent with their inhibitory activity toward NF-κB, compounds **1**, **2**, **7**, and **10** significantly inhibited the induction of COX-2 and iNOS mRNA in a dose-dependent manner (Figure 5), indicating that these compounds reduced the transcription of these genes. Moreover, the housekeeping protein β-actin was unchanged by the presence of compounds **1**, **2**, **7**, and **10** at the same concentration (Figure 5).

Currently, PPARs are therapeutic targets in the design and development of agonists for the treatment of type 2 diabetes and metabolic syndrome. The effects of compounds **1**−**16** on the PPARs activation were evaluated using a PPRE luciferase reporter assay. The results showed that compounds **1**−**5**, **7**, **9**, **10**, and **12**−**14** significantly activated PPARs transcriptional activity in a dose-dependent manner (Figure 6), with EC_{50} values ranging from 0.7 to 12.8 μM. Compounds **6**, **11**, **15**, and **16** displayed moderate activity, with EC_{50} values in a range of 16.8−21.6 μM, whereas compound **8** was not active at the tested concentrations (Table 3). Remarkably, compound **3** was the most effective and was even more potent than the positive control, benzafibrate (IC_{50} = 1.1 μM). From these primary data, with the aim of understanding how specifically the compounds modulate PPAR transcriptional activity, the PPAR transactivational effects of the isolated compounds were further examined on individual PPAR subtypes, including PPARα, -γ, and -$\beta(\delta)$ (Figures 7−9).

PPARα agonists have been reported to decrease hepatic, muscle, and pancreas lipotoxicity (steatosis), reduce insulin resistance, normalize glucose levels, and reduce cardiovascular risk factors such as dyslipidemia, inflammation, prothrombotic states, and intima-media thickness.[31] The effects of compounds **1**−**16** on PPARα activation were evaluated using a GAL-4-PPARα chimera assay. Among the compounds tested, compounds **2**, **3**, and **12** exhibited significant dose-dependent PPARα transactivational activity, with EC_{50} values of 7.0, 3.3, and 10.1 μM, respectively (Table 3). Compounds **1**, **4**−**7**, **9**−**11**, and **13**−**15** increased the transcriptional activity of PPARα, with EC_{50} values from 12.4 to 20.0 μM.

Among PPARs, PPARγ is the predominant molecular target for insulin-sensitizing thiazolidinedione drugs such as troglitazone, pioglitazone, and rosiglitazone, which have been approved for use in the treatment of type 2 diabetes.[32,33] The effects of compounds **1**−**16** on PPARγ activation were evaluated using a GAL-4-PPARγ chimera assay. The results showed that compounds **1**−**3** showed significant activity, with EC_{50} values of 11.9, 11.0, and 15.3 μM, respectively (Table 3).

Currently, PPAR$\beta(\delta)$ has become a pharmacological target for the treatment of metabolic disorders associated with metabolic syndromes, including dyslipidemia, obesity, and insulin resistance.[31] The use of two synthetic selective agonists, GW501516 and GW610742, in animal and various cell line models, and the concomitant development of new genetically modified mouse models, are helping to unravel the role of PPAR$\beta(\delta)$ in lipid and glucose homeostasis and inflammation. The effects of compounds **1**−**16** on PPAR$\beta(\delta)$ activation were evaluated using a GAL-4-PPAR$\beta(\delta)$ chimera assay. Among the compounds tested, compounds **1** and **3** significantly increased PPAR$\beta(\delta)$ transactivational activity, with EC_{50} values of 10.7 and 11.2 μM, respectively (Table 3).

PPARα/γ, PPAR$\gamma/\beta(\delta)$ dual, and PPAR$\alpha/\gamma/\beta(\delta)$ agonist combinations can achieve a broad spectrum of metabolic effects, reduce undesired weight gain and mortality rates by improving insulin sensitization, decreasing obesity, dyslipidemia, and hypertension, and provide beneficial effects on inflammatory markers.[12] Thus, the discovery and development of PPAR subtype combinations such as PPARα/γ and $\gamma/\beta(\delta)$ dual agonists and PPAR$\alpha/\gamma/\beta(\delta)$ agonists are ongoing. From the results, we found that compounds **1** and **3** had significant effects on the transactivational activities of three PPAR subtypes, while compound **2** exhibited significant effects on both PPARα and -γ transactivational activities, indicating that **2** acts as a PPARα/γ dual agonist. These data suggest that compounds **1**−**3** may be useful agents in the prevention and treatment of broad metabolic diseases.

In conclusion, this study describes the isolation of chemical components of the stem bark of *G. biloba*. Three new compounds, (2*E*,4*E*,1′*R*,3′*S*,5′*R*,8′*S*)-dihydrophaseic acid 3′-*O*-β-D-glucopyranoside, 7,8-dihydro-(*R*)-7-methoxyconiferyl alco-

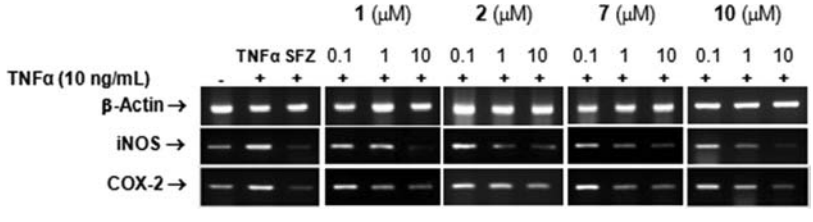

Figure 5. Effects of compounds **1**, **2**, **7**, and **10** on iNOS and COX-2 mRNA expression in HepG2 cells.

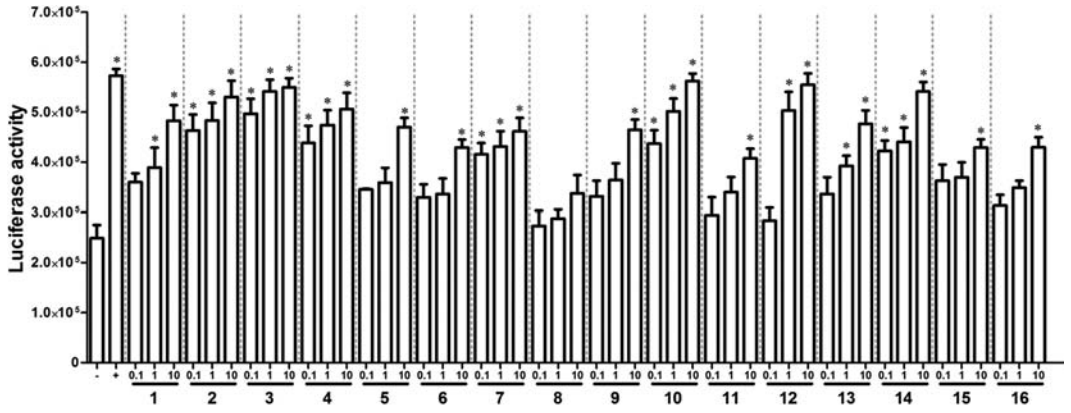

Figure 6. PPARs transactivational activity of compounds **1**−**16** in HepG2 cells. −, Vehicle group; +, positive control (1 μM): benzafibrate. *Significantly different from vehicle group ($P < 0.05$).

Table 3. PPARs, -α, -γ, and -$\beta(\delta)$ Transactivational Activities of Compounds 1−16[a]

	EC_{50} (μM)			
compd	PPARs	Gal4/PPARα-LBD	Gal4/PPARγ-LBD	Gal4/PPAR$\beta(\delta)$-LBD
1	10.4 ± 1.2	12.4 ± 1.7	11.9 ± 1.4	10.7 ± 1.5
2	3.0 ± 0.6	7.0 ± 1.3	11.0 ± 1.2	>30
3	0.7 ± 0.2	3.3 ± 0.8	15.3 ± 1.5	11.2 ± 0.9
4	5.6 ± 1.1	15.5 ± 2.1	>30	>30
5	12.4 ± 2.4	15.7 ± 2.6	>30	>30
6	18.0 ± 1.5	14.7 ± 2.0	29.6 ± 3.6	>30
7	10.9 ± 2.3	13.4 ± 1.8	>30	>30
8	>30[b]	>30	21.9 ± 2.3	29.3 ± 3.5
9	12.8 ± 1.4	16.2 ± 2.3	>30	>30
10	1.6 ± 0.4	17.0 ± 1.8	>30	>30
11	21.6 ± 2.1	22.0 ± 2.1	>30	>30
12	2.5 ± 0.6	10.1 ± 1.5	>30	>30
13	10.9 ± 1.1	20.0 ± 2.2	>30	>30
14	4.7 ± 0.8	19.6 ± 3.0	>30	>30
15	16.8 ± 1.7	18.4 ± 2.7	>30	>30
16	17.6 ± 1.5	28.3 ± 2.4	>30	>30
benzafibrate	1.1 ± 0.3			
ciprofibrate		0.9 ± 0.2		
troglitazone			0.8 ± 0.1	
L-165041				0.60 ± 0.07

[a]EC_{50}, the concentration of tested compound that gave 50% of the maximal reporter activity. [b]A compound was considered inactive with $EC_{50} > 30$ μM. The values are means ± SDs ($n = 3$).

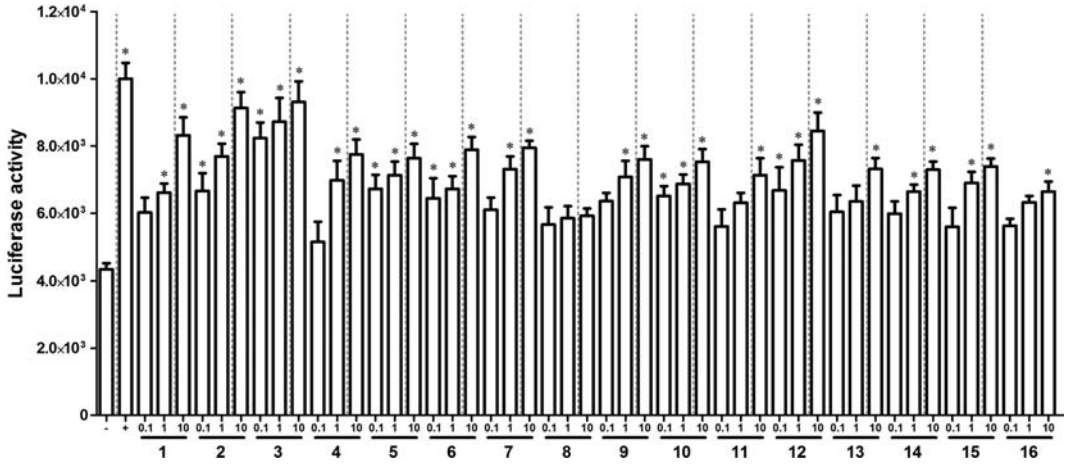

Figure 7. PPARα transactivational activity of compounds **1**−**16** in HepG2 cells. −, Vehicle group; +, positive control (1 μM): ciprofibrate. *Significantly different from vehicle group ($P < 0.05$).

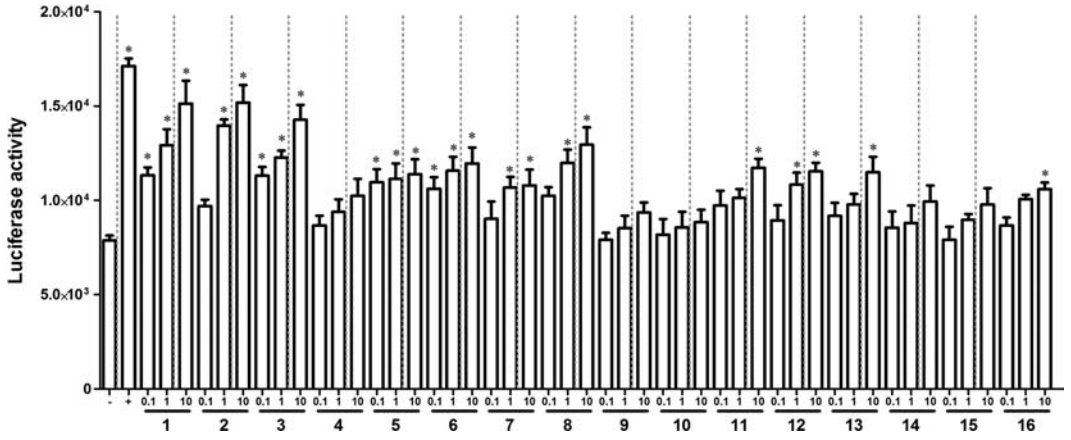

Figure 8. PPARγ transactivational activity of compounds **1**−**16** in HepG2 cells. −, Vehicle group; +, positive control (1 μM): troglitazone. *Significantly different from vehicle group ($P < 0.05$).

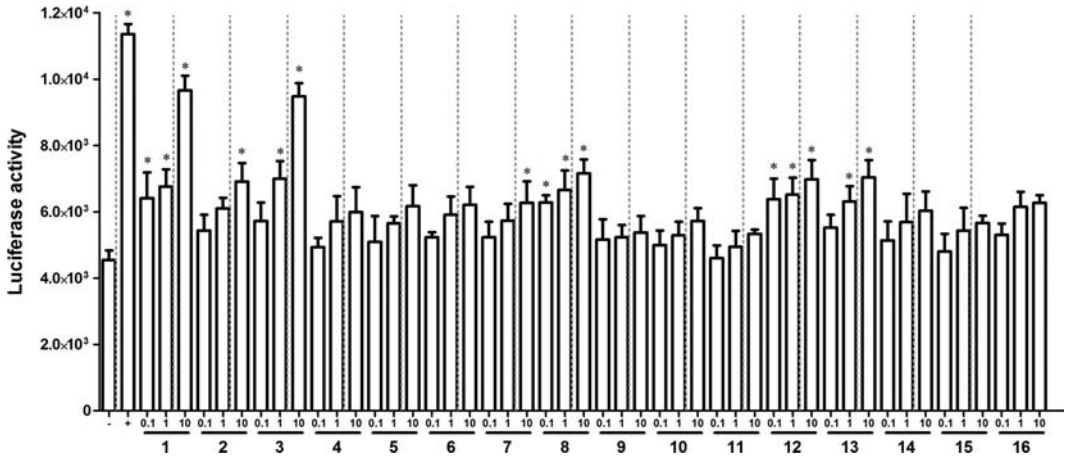

Figure 9. PPAR$\beta(\delta)$ transactivational activity of compounds **1**−**16** in HepG2 cells. −, Vehicle group; +, positive control (1 μM): L-165041. *Significantly different from vehicle group ($P < 0.05$).

hol, and (8*S*)-3-methoxy-8,4′-oxyneolignan-4,9,9′-triol 3′-*O*-β-D-glucopyranoside, were discovered. The effects of the isolated compounds on in vitro anti-inflammatory and PPAR transactivational pathways were investigated. These results provide scientific support for the use of *G. biloba* stem bark in the prevention and treatment of inflammatory and metabolic diseases. On the basis of these findings, additional studies of the potential of *G. biloba* stem bark in function foods are warranted. Cell viability, as measured by the MTT [3-(4,5-dimethylthiazole-2-yl)-2,5-diphenyltetrazolium bromide] colorimetric method,[34] showed that compounds **1**−**16** had no significant cytotoxicity in HepG2 cells at tested concentrations (data not shown).

■ ASSOCIATED CONTENT

Ⓢ Supporting Information

FTIR, NMR, and MS spectra of three new compounds (**1**−**3**). This material is available free of charge via the Internet at http://pubs.acs.org.

■ AUTHOR INFORMATION

Corresponding Author

*Tel: +82-42-821-5933. Fax: +82-42-823-6566. E-mail: yhk@cnu.ac.kr.

Funding

This study was supported by Priority Research Center Program through the National Research Foundation of Korea (NRF) funded by the Ministry of Education, Science and Technology (2009-0093815), Republic of Korea.

Notes

The authors declare no competing financial interest.

■ REFERENCES

(1) Joyeux, M.; Lobstein, A.; Anton, R.; Mortier, F. Comparative antilipoperoxidant, antinecrotic and scavenging properties of terpenes and biflavones from ginkgo and some flavonoids. *Planta Med.* **1995**, *61*, 126−129.

(2) Sticher, O. Quality of Ginkgo preparations. *Planta Med.* **1993**, *59*, 2−11.

(3) Singh, B.; Kaur, P.; Gopichand; Singh, R. D.; Ahuja, P. S. Biology and chemistry of *Ginkgo biloba*. *Fitoterapia* **2008**, *79*, 401−418.

(4) Mahadevan, S.; Park, Y. Multifaceted therapeutic benefits of *Ginkgo biloba* L.: Chemistry, efficacy, safety, and uses. *J. Food Sci.* **2008**, *73*, R14−R19.

(5) Pande, V.; Ramos, M. J. NF-kB in human disease: current inhibitors and prospects for de novo structure based design of inhibitors. *Curr. Med. Chem.* **2005**, *12*, 357−374.

(6) Baldwin, A. S. Jr. Series introduction: The transcription factor NF-kB and human disease. *J. Clin. Invest.* **2001**, *107*, 3−6.

(7) Berger, J.; Moller, D. E. The Mechanisms of action of PPARs. *Annu. Rev. Med.* **2002**, *53*, 409−435.

(8) Balint, B. L.; Nagy, L. Selective modulators of PPAR activity as new therapeutic tools in metabolic diseases. *Endocr., Metab. Immune Disord.: Drug Targets* **2006**, *6*, 33−43.
(9) Barish, G. D.; Narkar, V. A.; Evans, R. M. PPAR*d*: A dagger in the heart of the metabolic syndrome. *J. Clin. Invest.* **2006**, *116*, 590−597.
(10) Haluzik, M. M.; Haluzik, M. PPAR-*a* and insulin sensitivity. *Physiol. Res.* **2006**, *55*, 115−122.
(11) Kuroda, M.; Mimaki, Y.; Honda, S.; Tanaka, H.; Yokota, S.; Mae, T. Phenolics from *Glycyrrhiza glabra* roots and their PPAR-g ligand-binding activity. *Bioorg. Med. Chem.* **2010**, *18*, 962−970.
(12) Shearer, B. G.; Billin, A. N. The next generation of PPAR drugs: Do we have the tools to find them? *Biochim. Biophys. Acta, Mol. Cell. Biol. Lipids* **2007**, *1771*, 1082−1093.
(13) Kim, K. K.; Park, K. S.; Song, S. B.; Kim, K. E. Up regulation of GW112 Gene by NFkB promotes an antiapoptotic property in gastric cancer cells. *Mol. Carcinog.* **2010**, *49*, 259−270.
(14) Challice, J. S.; Loeffler, R. S. T.; Williams, A. H. Phenolic compounds of the genus *Pyrus*. Part 8. Structure of calleryanin and its benzylic esters from *Pyrus* and *Prunus*. *Phytochemistry* **1980**, *19*, 2435−2437.
(15) Pan, H.; Lundgren, L. N. Phenolic extractives from root bark of *Picea abies*. *Phytochemistry* **1995**, *39*, 1423−1428.
(16) Kanho, H.; Yaoya, S.; Kawahara, N.; Nakane, T.; Takase, Y.; Masuda, K.; Kuroyanagi, M. Biotransformation of benzaldehyde-type and acetophenone-type derivatives by *Pharbitis nil* hairy roots. *Chem. Pharm. Bull.* **2005**, *53*, 361−365.
(17) Yeo, H.; Chin, Y. W.; Park, S. Y.; Kim, J. Lignans of *Rosa multiflora* roots. *Arch. Pharm. Res.* **2004**, *27*, 287−290.
(18) Deyama, T.; Ikawa, T.; Nishibe, S. The constituents of *Eucommia ulmoides* Oliv. II. Isolation and structures of three new lignan glycosides. *Chem. Pharm. Bull.* **1985**, *33*, 3651−3657.
(19) Tokuoka, Y.; Daigo, K.; Takemoto, T. Constituents of *Epimedium*. III. Lignoids of *Epimedium grandiflorum*. *Yakugaku Zasshi* **1975**, *95*, 557−563.
(20) Fonseca, S. F.; Campello, J. d. P.; Barata, L. E. S.; Ruveda, E. A. ^{13}C NMR spectral analysis of lignans from *Araucaria angustifolia*. *Phytochemistry* **1978**, *17*, 499−502.
(21) Deyama, T. The Constituents of *Eucommia ulmoides* OLIV. I. Isolation of (+)-Medioresinol Di-O-b-D-glucopyranoside. *Chem. Pharm. Bull.* **1983**, *31*, 2993−2997.
(22) Li, H. Z.; Luo, G. J.; Li, H. M.; Li, X. L.; Liz, R. T. A new aryltetrahydronaphthalene lignan from *Epimedium brevicornum*. *Chin. Chem. Lett.* **2011**, *22*, 85−87.
(23) Lee, H.-J.; Lee, H.-J.; Je, K.-H.; Seo, J. K.; Lee, S. J.; Bang, S. L. Novel compound isolated from *Ginkgo biloba* bark, isolation method thereof and antiplatelet composition containing the same. *U.S. Pat. Appl. Publ.* **2008**, 14.
(24) van Beek, T. A. Ginkgolides and bilobalide: Their physical, chromatographic and spectroscopic properties. *Bioorg. Med. Chem.* **2005**, *13*, 5001−5012.
(25) del Refugio Ramos, M.; Jerz, G.; Villanueva, S.; Lopez-Dellamary, F.; Waibel, R.; Winterhalter, P. Two glucosylated abscisic acid derivates from avocado seeds (*Persea americana* Mill. Lauraceae cv. Hass). *Phytochemistry* **2004**, *65*, 955−962.
(26) Lutz, A.; Winterhalter, P. Abscisic alcohol glucoside in quince. *Phytochemistry* **1992**, *32*, 57−60.
(27) Baba, H.; Yaoita, Y.; Kikuchi, M. Constituents of the roots of *Ligularia dentata* Hara. *J. Nat. Med.* **2007**, *61*, 472−473.
(28) Kim, K. H.; Kim, H. K.; Choi, S. U.; Moon, E.; Kim, S. Y.; Lee, K. R. Bioactive lignans from the rhizomes of *Acorus gramineus*. *J. Nat. Prod.* **2011**, *74*, 2187−2192.
(29) Wong, H. R.; Menendez, I. Y. Sesquiterpene lactones inhibit inducible nitric oxide synthase gene expression in cultured rat aortic smooth muscle cells. *Biochem. Biophys. Res. Commun.* **1999**, *262*, 375−380.
(30) Pahl, H. L. Activators and target genes of Rel/NF-kB transcription factors. *Oncogene* **1999**, *18*, 6853−6866.
(31) Gross, B.; Staels, B. PPAR agonists: Multimodal drugs for the treatment of type-2 diabetes. *Best Pract. Res., Clin. Endocrinol. Metab.* **2007**, *21*, 687−710.
(32) Kaplan, F.; Al-Majali, K.; Betteridge, D. J. PPARS, insulin resistance and type 2 diabetes. *J. Cardiovasc. Risk* **2001**, *8*, 211−217.
(33) Moller, D. E. New drug targets for type II diabetes and the metabolic syndrome. *Nature* **2001**, *414*, 821−827.
(34) Scudiero, D. A.; Shoemaker, R. H.; Paull, K. D.; Monks, A.; Tierney, S.; Nofziger, T. H.; Currens, M. J.; Seniff, D.; Boyd, M. R. Evaluation of a soluble tetrazolium/formazan assay for cell growth and drug sensitivity in culture using human and other tumor cell lines. *Cancer Res.* **1988**, *48*, 4827−4833.